

Environmental Research Letters



LETTER

Variability of fire emissions on interannual to multi-decadal timescales in two Earth System models

OPEN ACCESS

RECEIVED

29 April 2016

REVISED

14 November 2016

ACCEPTED FOR PUBLICATION

22 November 2016

PUBLISHED

2 December 2016

Original content from this work may be used under the terms of the [Creative Commons Attribution 3.0 licence](#).

Any further distribution of this work must maintain attribution to the author(s) and the title of the work, journal citation and DOI.

D S Ward¹, E Shevliakova², S Malyshev², J-F Lamarque³ and A T Wittenberg⁴¹ Program in Atmospheric and Oceanic Sciences, Princeton University, Princeton, NJ, USA² Department of Ecology and Evolutionary Biology, Princeton University, Princeton, NJ, USA³ National Center for Atmospheric Research, Boulder, CO, USA⁴ NOAA/Geophysical Fluid Dynamics Laboratory, Princeton, NJ, USAE-mail: dward@princeton.edu**Keywords:** climate variability, fire emissions, Earth system modelsSupplementary material for this article is available [online](#)**Abstract**

Connections between wildfires and modes of variability in climate are sought as a means for predicting fire activity on interannual to multi-decadal timescales. Several fire drivers, such as temperature and local drought index, have been shown to vary on these timescales, and analysis of tree-ring data suggests covariance between fires and climate oscillation indices in some regions. However, the shortness of the satellite record of global fire events limits investigations on larger spatial scales. Here we explore the interplay between climate variability and wildfire emissions with the preindustrial long control numerical experiments and historical ensembles of CESM1 and the NOAA/GFDL ESM2Mb. We find that interannual variability in fires is underpredicted in both Earth System models (ESMs) compared to present day fire emission inventories. Modeled fire emissions respond to the El Niño/southern oscillation (ENSO) and Pacific decadal oscillation (PDO) with increases in southeast Asia and boreal North America emissions, and decreases in southern North America and Sahel emissions, during the ENSO warm phase in both ESMs, and the PDO warm phase in CESM1. Additionally, CESM1 produces decreases in boreal northern hemisphere fire emissions for the warm phase of the Atlantic Meridional Oscillation. Through analysis of the long control simulations, we show that the 20th century trends in both ESMs are statistically significant, meaning that the signal of anthropogenic activity on fire emissions over this time period is detectable above the annual to decadal timescale noise. However, the trends simulated by the two ESMs are of opposite sign (CESM1 decreasing, ESM2Mb increasing), highlighting the need for improved understanding, proxy observations, and modeling to resolve this discrepancy.

Introduction

Extreme fire emissions from Indonesia in 2015 were in the global news and were linked to major degradation of regional air quality (Chisholm *et al* 2016), which has been suggested to contribute to increased mortality in Southeast Asia (Marlier *et al* 2012). These fires were brought on by dry conditions associated with the strong 2015–2016 El Niño and, preliminarily, are thought to be the most extreme episode of fires in this region since the 1997–1998 El Niño and could bring even higher economic costs (Chisholm *et al* 2016).

Factors underlying fires in this region, especially exposure of large amounts of peat following forest clearing, exacerbate the potential severity of the burning and subsequent emissions (Marlier *et al* 2014, 2015), but it is natural climate variability that drives the timing and scale of these events (Chen *et al* 2011, 2016). Fire variability in other regions has also been connected to the El Niño/southern oscillation (ENSO) (e.g. Heyerdahl *et al* 2008, Le Page *et al* 2008, Monks *et al* 2012) and the Pacific decadal oscillation (PDO) (e.g. Duffy *et al* 2005, Kitzberger *et al* 2007). The impacts of these variations are felt

globally; for example, fires are the main cause of interannual variability (IAV) in global carbon monoxide concentrations and carbonaceous aerosol optical depth (Voulgarakis *et al* 2015), with implications for global atmospheric chemistry, cloud physics, and radiative forcing (e.g. Naik *et al* 2005, Randerson *et al* 2006, Ward *et al* 2012, Tosca *et al* 2015), and also play an important role in the variable annual growth rate of CO₂ (Nevison *et al* 2008).

Despite the clear connection between Pacific sea surface temperature (SST) anomalies and fires in equatorial Asia, our understanding of these relationships on a global scale and for regions without long observational records of fires (including much of the tropics and subtropics) is limited by the length of the satellite record in which active fires can be sensed remotely, roughly 18 years (Giglio *et al* 2013). Moreover, there are reasons to suspect that global fires exhibit decadal and multidecadal variability because important fire drivers have been shown to vary on these timescales, including precipitation and soil water (Ault *et al* 2012, 2013, Dai 2012, Chikamoto *et al* 2015), temperature (Meehl 2015), and ENSO itself, which may undergo periods of extreme behavior on a wide range of timescales (Wittenberg 2009, 2015, Emile-Geay *et al* 2013, McGregor *et al* 2013, Wittenberg *et al* 2014, Capotondi *et al* 2015). While the satellite record of fires is too short to fully characterize variability on decadal timescales, charcoal sediment records, used as a proxy for fire emissions, cover much longer time periods but typically with century-averaged values that do not provide information on multidecadal aspects (e.g. Marlon *et al* 2008, Daniu *et al* 2012). An alternate proxy for fire activity, burn scars on tree rings, has been used to suggest a connection between decadal climate oscillations and fires in western North America (Kitzberger *et al* 2007, Taylor *et al* 2008, Trouet *et al* 2010). Ice core records of black carbon deposition and trace gas tracers for fire activity (e.g. Zennaro *et al* 2014) have not been utilized for this purpose to our knowledge, but could provide higher time resolution than charcoal sediments (Bauer *et al* 2013).

The gap in our knowledge of interactions between climate variability and fires on a global scale spans timescales that are important for near-term predictions, and limits our ability to address questions of detection and attribution. With the lack of available observational data of sufficient length, Earth System models (ESMs), which account for interactions among multiple fire drivers, may be used to provide information about how fires respond regionally and globally to variations in climate across timescales. Numerical experiments with CO₂-concentration driven ESMs allow a separation between forced signal (e.g. historical warming or land use and land cover change) and internal climate variability. In this study we investigate fires in long model integrations with preindustrial forcing, as well as ensemble simulations of the historical

time period using the Community Earth System Model (CESM1) (Hurrell *et al* 2013, Kay *et al* 2015) and the Geophysical Fluid Dynamics Laboratory (GFDL) ESM2Mb (Dunne *et al* 2012, Malyshev *et al* 2015). We aim to characterize the role of internal climate variability (Baede *et al* 2001) in driving fires in order to inform future modeling investigations of fire regime changes, extreme events and trend detection.

Methods

The CESM1 Large Ensemble Community Project (LENS) comprises historical and future simulations with many ensemble members, with an aim of improving our ability to distinguish between climate change and climate variability. Kay *et al* (2015) provide a detailed description of the LENS simulation protocol. In this project, the CESM1 land, ocean, atmosphere and sea-ice components have approximately 1° resolution and it was forced with 1850 solar and radiative forcing and 1850 land cover for the preindustrial control. We use the last 1800 years of the CESM1 control simulation and also examine the 40 members of the CESM1 historical ensemble from years 1920 to 2005. The ensemble members are initialized with slightly perturbed initial conditions to provide a sampling of internal climate variability under historical climate forcing. Land cover change in the 20th century ensemble is represented by plant functional type (PFT) transitions on a yearly basis and follows Hurtt *et al* (2011), adjusted to match the CESM1 land model PFT scheme by Lawrence *et al* (2012).

The CESM1 fire model is based on the Thonicke *et al* (2001) scheme, which simulates fires on a daily basis. In this scheme, probability of fire occurrence is parameterized as a function of soil moisture in the top 0.5 m of the soil, with separate ‘moisture of extinction’ values for woody and herbaceous PFTs above which fires will not occur. Fire occurrence in this model requires dead litter availability above 100 gC m⁻² and also a ground temperature above zero Celsius (Thonicke *et al* 2001). Fire season length and annual area burned are computed from an empirically-derived fuel moisture function (Thonicke *et al* 2001). Carbon (C) emissions from fires are determined by applying PFT-specific combustion completeness and mortality factors to the available biomass within the burned area.

ESM2Mb is based on ESM2M (Dunne *et al* 2012, 2013) with updated parameter settings for the land model LM3 (Malyshev *et al* 2015), approximately 2° horizontal resolution for the atmosphere and land, and roughly 1° horizontal resolution for sea-ice and ocean components. The control run was continued for 6000 model years after reaching quasi-equilibrium with solar and radiative forcing representative of year 1860. This simulation used potential vegetation (i.e. undisturbed by human land use) instead of

preindustrial vegetation cover and includes dynamic vegetation, important distinctions from the CESM1 control run. In addition to the preindustrial control, we analyze the corresponding 10-member ensemble of historical forcing simulations running from 1861 to 2005 with 20th century land cover changes following Hurtt *et al* (2011). The ESM2Mb transitions from potential vegetation in the preindustrial control run to 1861 land cover via a 160 year 'bridge' experiment with 1860 radiative forcing and 1700–1860 land cover historical reconstructions (Hurtt *et al* 2011).

The ESM2Mb fire model, described by Shevliakova *et al* (2009), predicts fires as a function of soil moisture but fires occur annually. Under this scheme, individual months are designated as drought or non-drought, based on the soil moisture deficit. The yearly sum of drought months and the available above ground fuel are used to modulate a PFT-specific climatological fire return-interval factor that yields annual fire emissions of C at each grid point (Shevliakova *et al* 2009). In contrast to CESM1, this scheme is bound more to the seasonal cycle of soil moisture and fuel availability and has no direct air temperature-dependence.

The fire models used in this study do not capture subtle ecosystem shifts that impact fire dynamics, such as different species make-up within similar PFTs (Kelly *et al* 2013, Rogers *et al* 2015), or landscape fragmentation (Nepstad *et al* 2006, Chen *et al* 2013). In addition, neither fire model explicitly simulates fire ignition from lightning or human activity, which is often represented in global fire models (e.g. Kloster *et al* 2010, Li *et al* 2013, Pfeiffer *et al* 2013, Yue *et al* 2014, Le Page *et al* 2015). Recent studies indicate a diminished role for natural (Bistinas *et al* 2014) and anthropogenic (Prentice *et al* 2011) ignitions in global fire prediction. Lightning, however, may be a better predictor of fire on a regional basis (Abatzoglou *et al* 2016). Moreover, lightning has been shown to vary substantially with tropical Pacific SST anomalies (Sátori *et al* 2009). We are unable to explore any connections between IAV in lightning and fires with the current model setup. Models that include lightning ignitions typically use a lightning climatology and are, therefore, also unable to explore these connections.

Our analysis of fire emissions from both ESMs is done on an annual basis. Fires in some arid regions respond to the robustness of the previous wet season and associated vegetation growth (Van der Werf *et al* 2008). We shift the start month of the annual averages for CESM1 emissions at each grid point to eight months prior to the model climatological peak in fire emissions, determined by harmonic analysis, to account for the different regional seasonality. Annual windows for locations with biannual fire cycles were not shifted. This shifting is applied in the ENSO composite analysis only.

We use the GFED4s (Giglio *et al* 2013), GFASv1 (Kaiser *et al* 2012) and FINN (Wiedinmyer *et al* 2011)

fire emission inventories (details in supplementary material) for comparison to present-day model fire emission variability for 14 regions (figure S1). In addition, we compiled charcoal sedimentation records from the Global Charcoal Database (GCD) for 11 sites in western North America (table S1) (Power *et al* 2008) as a proxy for past fire emissions in this region (details in supplementary material). We note that as a metric of fire activity, C emissions emphasize forest fires, while another commonly used measure, area burned, is dominated by savannah and grassland fires (van der Werf *et al* 2008).

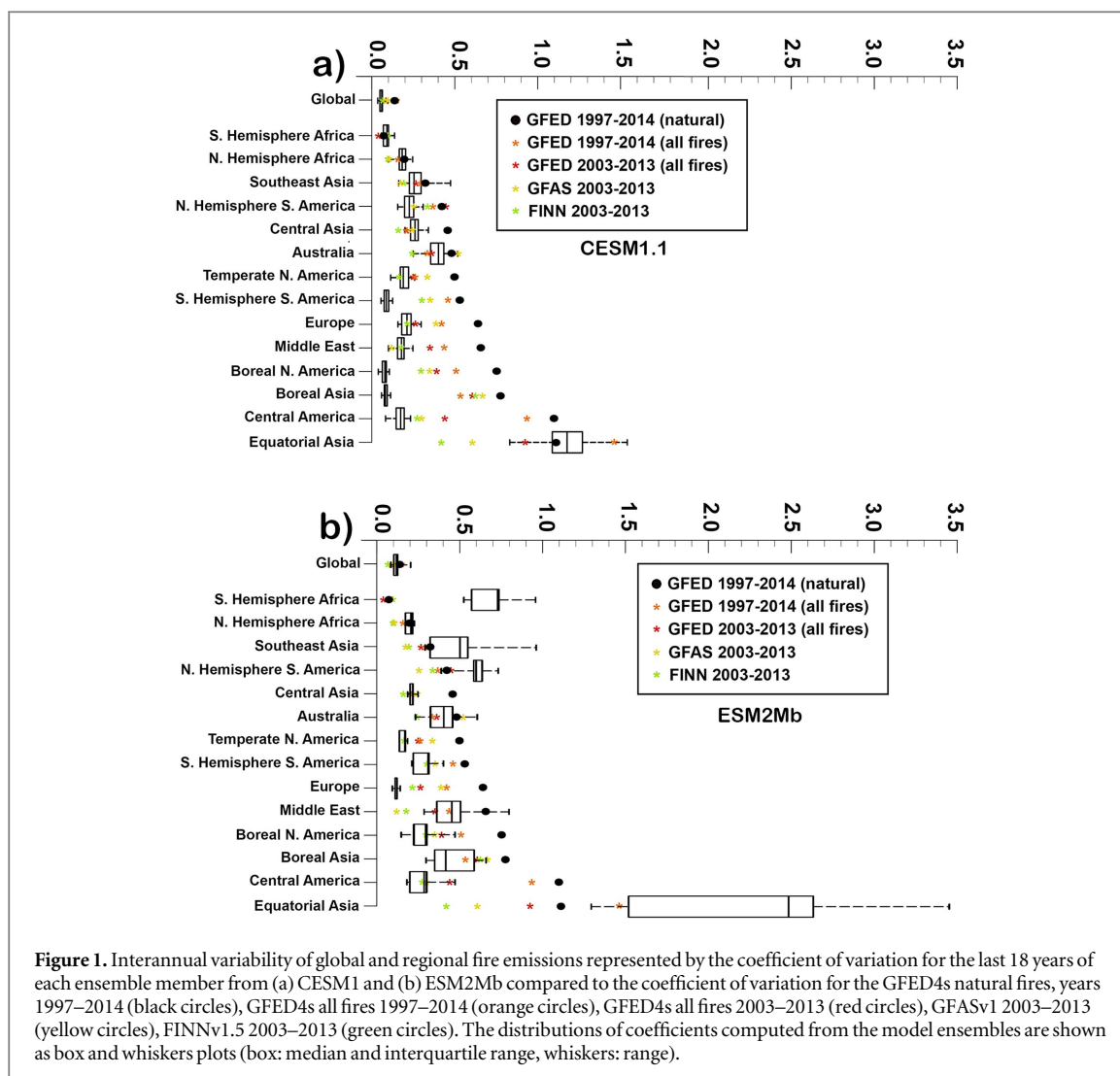
To compute ENSO indices we use SSTs averaged over the NINO3 region (150W–90W, 5S–5N), as in Wittenberg (2009), for which positive values indicate El Niño-like conditions and negative values indicate La Niña-like conditions. Both ESMs generate a reliable ENSO with ESM2Mb producing a stronger ENSO compared to CESM1 and the HadISST1 timeseries (Rayner *et al* 2003) (figure S2). Precipitation teleconnection patterns are similar between the two models for North America and equatorial Asia but show substantial differences in both the sign and seasonal timing of the response in Africa (figure S3).

We quantify the interdecadal Pacific oscillation (IPO) index as the leading principal component of Pacific basin SSTs after applying a 13 year low-pass filter to the unforced long-control model run (Meehl *et al* 2009). We split the model timeseries into periods of 300 years before filtering and computing the empirical orthogonal functions. For CESM1, the first EOF explains 39% of the variance and exhibits a spatial pattern very similar to the IPO associated with observed SSTs (not shown) suggesting that the model captures this mode of interdecadal variability. For ESM2Mb, the first EOF explains less than 25% of the variance. Therefore, we do not use the IPO index computed from the ESM2Mb in the remainder of the study. Hereafter we refer to this index as the PDO, noting that the IPO and PDO are highly correlated and the terms are often used interchangeably (Meehl 2015).

The Atlantic Meridional Oscillation index is here defined as the SST anomalies in the North Atlantic Ocean (80W–0W, 0N–60N) minus global SST anomalies (60S–60N), following Trenberth and Shea (2006) as recommended by Phillips *et al* (2014). We also compute 10 year and 50 year low-pass filtered AMO index timeseries, as in Knight *et al* (2006), to remove variability related to ENSO and the PDO, respectively.

Results

We assess the IAV in fire emissions globally and by region using the coefficient of variation (CV; quotient of the standard deviation and the mean) (figure 1). Globally, CESM1 and ESM2Mb underpredict the CV in comparison to the GFED4s natural fires. The largest regional biases occur in boreal regions where fires are



more episodic than in the tropics (Clark *et al* 2015). Precipitation is not underestimated in boreal regions (figure S4), suggesting the bias is caused by poor representation of other fire drivers, such as ignition and temperature, which are more important in boreal zones. Temperature, for example, drives boreal fire season length and severity (Flannigan *et al* 2009) and the depth of the active layer of permafrost, which regulates area burned and fire severity (e.g. Venevsky 2001, Froking *et al* 2011). Central American fires increased strongly with the 1997–98 El Niño (van der Werf *et al* 2004) but here both models show positive and negative precipitation responses to ENSO in this region (figure S3), dampening any model response in fire emissions. The full GFED4s record has generally higher CV than the 2003–2013 record (figure 1), likely due to the influence of the 1997–98 El Niño. Also, the addition of anthropogenic fires (largely deforestation and agricultural fires) leads to lower CV in the GFED4s and ostensibly in the GFASv1 and FINNv1.5 as well (figure 1). Both the CESM1 and ESM2Mb capture the high variability in equatorial Asia, attributable largely to extreme responses to the dry conditions associated with the 1997–98 El Niño

event (van der Werf *et al* 2004, 2006, Giglio *et al* 2013), suggesting that the models demonstrate some response to ENSO.

The power spectrum of CESM1 fire emissions shows substantial variance at periods of 3–7 years, which is significantly different from red noise at a 95% confidence level (figure 2(a)). The variance of ESM2Mb fire emissions is not clearly distinguishable from red noise at any frequency, although the signal is strongest for periods of 3–7 years (figure 2(b)). Individual regions show statistically significant variance at these timescales, including temperate North America in both ESMs, and all Asian regions in CESM1 (figures 2(a), (b)). In the CESM1 output, variance is distinguishable from red noise in southern hemisphere Africa and the Middle East on timescales of the PDO (10–30 years), and in Central America and boreal N America on AMO timescales (75–100 years) (figures 2(a), (d)).

The shortness of the GFED4s record of fire emissions makes it difficult to interpret its power spectrum (figure 2(c)). There is a suggested connection to ENSO with higher variance at a period of 5 years but this periodicity cannot be confirmed statistically with the small

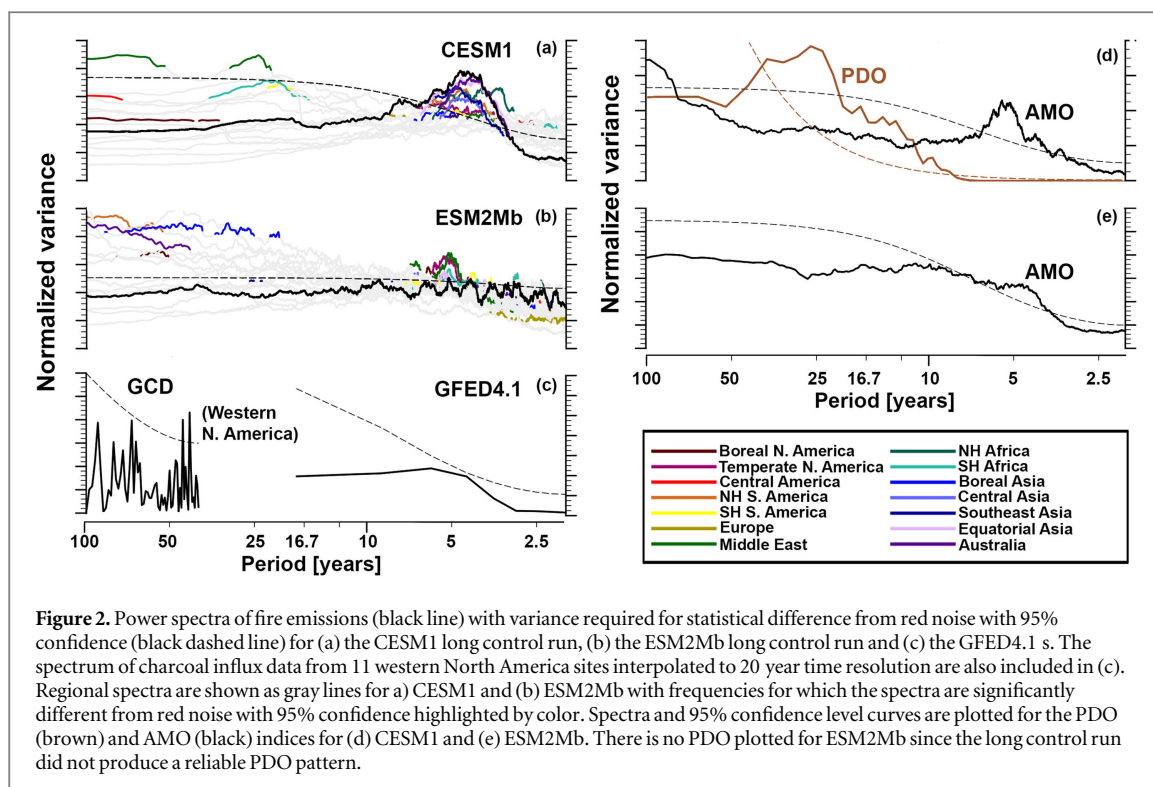


Figure 2. Power spectra of fire emissions (black line) with variance required for statistical difference from red noise with 95% confidence (black dashed line) for (a) the CESM1 long control run, (b) the ESM2Mb long control run and (c) the GFED4.1 s. The spectrum of charcoal influx data from 11 western North America sites interpolated to 20 year time resolution are also included in (c). Regional spectra are shown as gray lines for a) CESM1 and (b) ESM2Mb with frequencies for which the spectra are significantly different from red noise with 95% confidence highlighted by color. Spectra and 95% confidence level curves are plotted for the PDO (brown) and AMO (black) indices for (d) CESM1 and (e) ESM2Mb. There is no PDO plotted for ESM2Mb since the long control run did not produce a reliable PDO pattern.

sample size. GCD timeseries from western North American sites exhibit strong variability at longer periods of about 40 years and 70 years (figure 2(c)). However, given our knowledge of variability associated with ENSO, it is possible that aliasing of higher frequency oscillations is responsible for some of the variance. The potential for aliasing is difficult to state with certainty given that the GCD data are accumulation rates, each encompassing several years, and have different original timesteps depending on the site. The problematic nature of spectral analysis on the available datasets of fire emissions and proxies stands to highlight the gaps in our knowledge of fire/climate interactions, especially on decadal timescales.

We assess the variability of fire emissions with the aforementioned climate oscillation indices using composite analysis. We group the long control run annual fire emissions by positive or negative index, ENSO, PDO and AMO, and compute the difference in means between the data subsets at each model grid point. A simple statistical test of difference between means is then applied to identify locations where the mean fire emissions shift depending on the sign of the oscillation index. The fire emissions timeseries are standardized such that the differences in mean are plotted as fractions of the standard deviation characteristic of each location. We present analysis of fire emissions relationship to the decadal and multi-decadal climate oscillations for CESM only because ESM2Mb does not generate a reliable PDO and does not produce an AMO with variability on multidecadal timescales (figure 2(e)).

The spatial pattern of the CESM1 response to ENSO (figure 3(a)) compares well to the fire emission anomalies observed during the 1997–1998 El Niño with anomalously high emissions in boreal North America, the Amazon, southeast Asia, and Australia, and decreased emissions in northern hemisphere Africa (van der Werf *et al* 2004) (figure S5). The ESM2Mb fire emissions exhibit a similar spatial pattern of response to ENSO but the signal is weak (figure 3(b)), as suggested by the spectral analysis (figure 2(b)).

The response of CESM1 fire emissions to the PDO index is weaker than the response to ENSO but follows a similar spatial pattern (figure 3(c)) except in boreal North America where fire emissions are negatively correlated with the PDO index. In this region, the average soil moisture increases for warm-phase PDO (not shown), contributing to a decrease in fires during this phase.

CESM1 fire emissions also exhibit a statistically significant response to different phases of the AMO in several regions (figure 3(d)). The abrupt change in sign of the response across the equator in South America, positive southward and negative northward (figure 3(d)), is consistent with analysis of satellite-derived fire counts from Chen *et al* (2011) who attribute the change to shifts in the ITCZ and precipitation climatology that are associated with the different phases of the AMO. In general, the CESM1 fire emissions response to the AMO is opposite in sign to the PDO response (figure 1(c)), which is consistent with drought and pluvial relationships between the PDO and AMO (e.g. Findell and Delworth 2010). However,

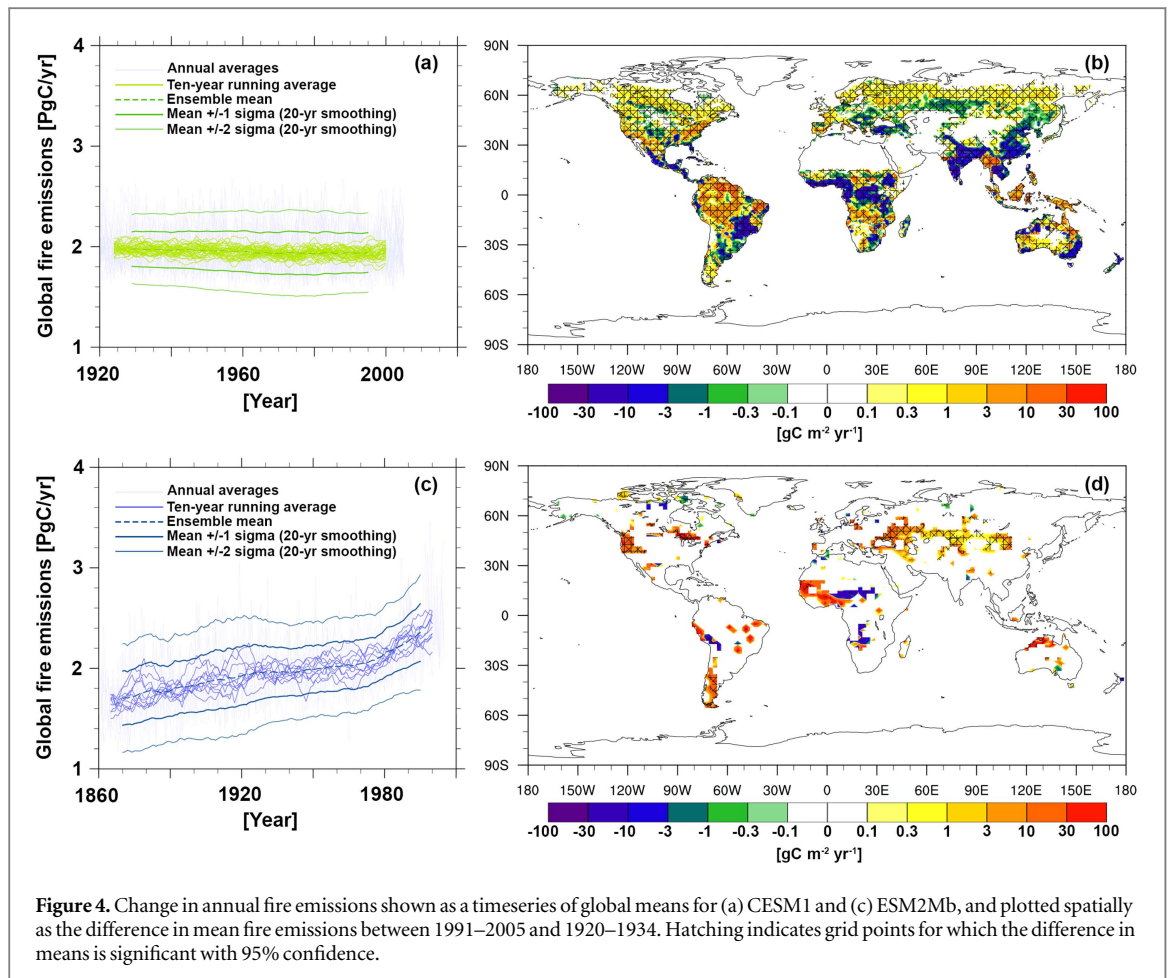
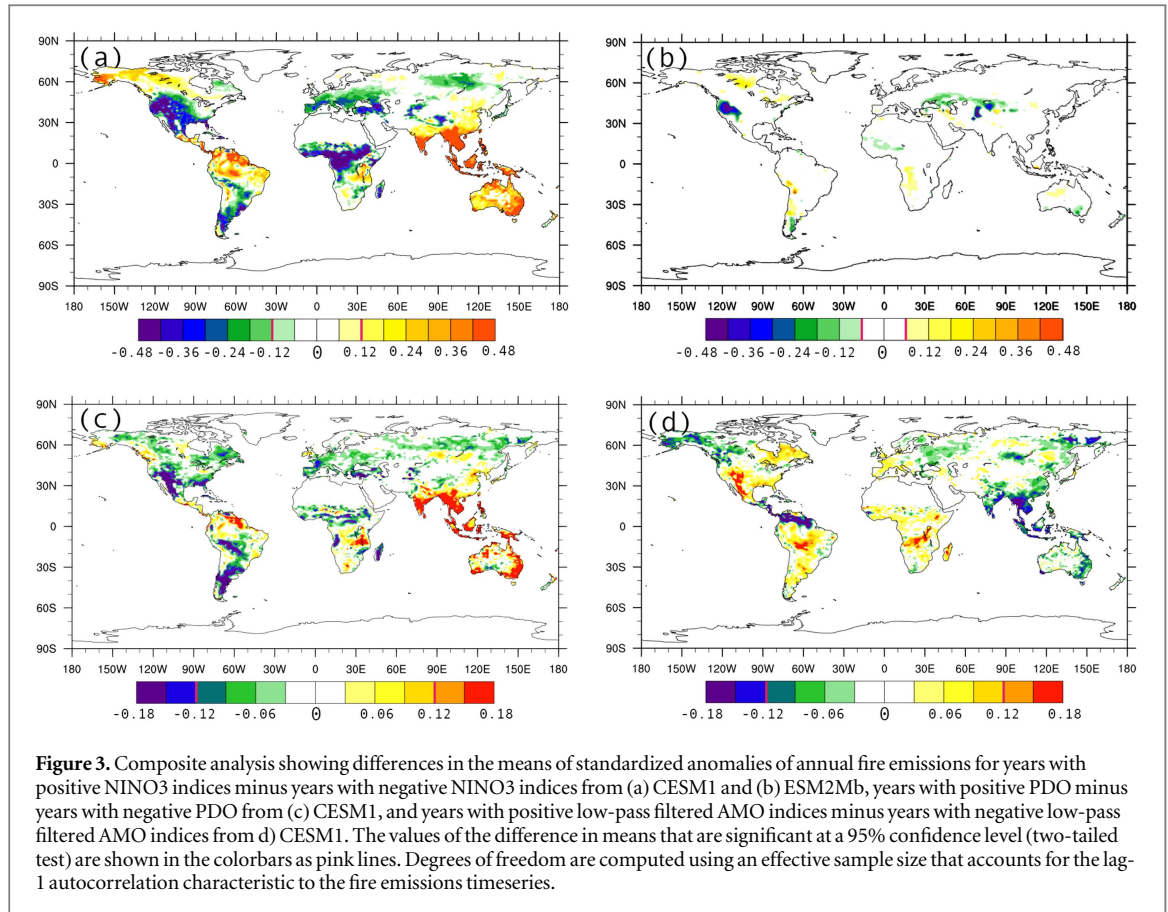


Table 1. Threshold for significance of trends in fire emissions. This is expressed as the difference in global fire emissions (TgC yr^{-1}) averaged over a given number of years that is detectable at a 95% statistical confidence level with the given number of model ensemble members. Values are based on the variance of the ESM2Mb and CESM1 long control simulations.

ESM2Mb								
Ensemble members	Number of years							
	3	5	10	15	18	20	50	100
3	542	418	296	246	223	215	141	116
5	247	191	135	112	102	98	65	53
10	134	104	73	61	55	53	35	29
20	86	66	47	39	35	34	22	18
30	68	52	37	31	28	27	18	14
40	48	37	26	22	20	19	13	10
CESM1								
Ensemble members	Number of years							
	3	5	10	15	18	20	50	100
3	301	223	157	132	114	108	52	32
5	137	102	71	60	52	49	24	15
10	75	55	39	33	28	27	13	8
20	48	35	25	21	18	17	8	—
30	38	28	20	16	14	14	6	—
40	27	20	14	12	10	10	—	—

several studies have shown that a positive AMO can enhance environmental conditions brought on by a positive phase of the PDO (e.g. Kitzberger *et al* 2007, Mo *et al* 2009). Applying a 50 year low-pass filter to the AMO index here reduces the strong tropical response in fire emissions to AMO (figure S6) implying a connection exists between the AMO and PDO in the model results.

The ESM2Mb ensemble mean fire emissions increase by about 400 TgC yr^{-1} between 1920 and 2005 while the CESM1 produces a small decrease ($\sim 25 \text{ TgC yr}^{-1}$) in 10 year mean over the same time period (figures 4(a), (c)). The divergence of the trends results from differences in the fire model response to environmental factors, such as temperature and precipitation, and differences in the ESM predictions of these environmental factors. Efforts to determine 20th century trends in fire activity from observations have also led to mixed results. Mouillot and Field (2005) compiled a detailed historical reconstruction of area burned by fires, combining satellite retrievals, field records, and tree-ring data. They conclude that global fires have increased since 1900, with a mid-century minimum in fire activity. However, it is difficult to compare their dataset with the model results reported here which do not account for deforestation fires or human fire ignition and suppression.

CESM1 exhibits a small global trend in fire emissions but there are major regional increases in the boreal northern hemisphere, equatorial Asia and much of the Amazon (figure 4(b)) that appear to be driven by land cover changes. Parts of southeast Asia underwent a transition from largely primary forest vegetation to herbaceous vegetation during the 20th century (Hurtt *et al* 2011), which reduces the moisture of extinction

for fires in the CESM1 fire scheme and also shrinks fuel availability, leading to reduced fire. In boreal forests, increasing temperatures lengthen the fire season in CESM1, enhancing fire emissions despite higher soil moisture.

Historical trends in emissions in ESM2Mb are largely driven by soil moisture changes. Where regional trends are statistically significant from 1920 to 2005 they are uniformly positive (figure 4(d)). The changes are related to increases in drought months over this time period, and enhanced in the western United States, central Asia, and southern South America by co-located increases in fuel availability.

Discussion and conclusions

Anthropogenic impacts on climate and land cover could have led to positive trends in 20th century global fire activity (Mieville *et al* 2010, Lasslop and Kloster 2015), negative trends (Marlon *et al* 2008, Yang *et al* 2014, Knorr *et al* 2016), or trends that change sign (Mouillot and Field 2005, Kloster *et al* 2010, Pechony and Shindell 2010). Here we are able to show that historical trends in fire emissions for CESM1 and ESM2Mb, while opposite in sign, are statistically significant at a 95% confidence level with a null hypothesis of zero trend. This is to say that a 20th century anthropogenic signal, including human impacts on climate, CO_2 , and land cover, is detectable in natural fires above the year-to-year noise in fire emissions in these two ESMs. The significance testing used here can be generalized to any size trend and number of ensemble members (table 1).

The magnitudes of significant trends differ substantially between the CESM1 and ESM2Mb due to

the dissimilar natural variability in fire emissions inherent to each model. The model dissimilarities could result from biases in fuel load and climate variability in the ESMs (figures S2, S3), and differences in model processes such as dynamic vegetation in ESM2Mb compared to static vegetation in CESM1. In more recent versions of CESM, the Thonicke *et al* (2001) fire model has been replaced with that of Li *et al* (2013), which represents peat and deforestation fires, as well as natural and human ignition and fire suppression, and is able to improve model reproduction of fire spatial patterns, total emissions, and IAV (Li *et al* 2013). Small-scale land cover effects on wildfires, such as ecosystem edge effects and local variations in surface hydrology, are still not well represented in global fire models (Ward and Mahowald 2015). These effects could be especially important in regions of intense land conversion, including equatorial Asia where, as mentioned in the Introduction, deforestation can expose massive amounts of peat and increase the sensitivity of regional fire emissions to climate variability (Marlier *et al* 2015). Greater attention to these small-scale, often sub-grid-scale, processes could improve our understanding of anthropogenic impacts on fire variability.

The spatial pattern of the fire emissions response to ENSO in both CESM1 and ESM2Mb is roughly consistent with observational records of fires in Canada (Skinner *et al* 2006) and Alaska (Hess *et al* 2001), and studies of tree-ring burn-scar synchrony. Greater synchrony, an indicator of increased fire activity (Falk *et al* 2011), occurs during the cold phase of ENSO in the southwest and interior west United States, and during the warm phase of ENSO in the Pacific northwest (Kitzberger *et al* 2007, Trouet *et al* 2010). Burn-scar synchrony studies of connections between fire activity and decadal oscillations, such as the PDO, are generally inconclusive due to uncertainties in the proxies of climate variability (Kipfmüller *et al* 2012), but possible connections would have major implications for decadal fire prediction on a global scale. For example, best estimates of global fire emissions, such as the GFED4s, are based on data collected almost entirely during a negative phase of the PDO, and there is evidence that a phase change may have occurred in 2014 (Meehl 2015).

Our results suggest that, with this phase change in the PDO, southeast Asia, Australia, the northern Amazon region, and eastern equatorial Africa will see a shift to higher fire emissions contributed by natural climate variability, and the southwestern United States, northern Mexico, and the southwestern Amazon will shift to lower fire emissions contributed by natural variability. Increasing confidence in long-term forecasts such as these will require further progress in our understanding of the natural variability in fires from additional observations and proxy data, as well as improved modeling of global fires.

Acknowledgments

We would like to acknowledge assistance from Jennifer Marlon for providing data from the GCD. Computing resources (ark:/85065/d7wd3xhc) were provided by the Climate Simulation Laboratory at NCAR's Computational and Information Systems Laboratory, sponsored by the National Science Foundation and other agencies. The CESM project is supported by the National Science Foundation and the Office of Science (BER) of the US Department of Energy. The National Science Foundation sponsors NCAR. This report was prepared by D Ward under award NA14OAR4320106 from the National Oceanic and Atmospheric Administration (NOAA), US Department of Commerce. The statements, findings, conclusions, and recommendations are those of the authors and do not necessarily reflect the views of NOAA, or the US Department of Commerce.

References

- Abatzoglou J T, Kolden C A, Balch J K and Bradley B A 2016 Controls on interannual variability in lightning-caused fire activity in the western US *Environ. Res. Lett.* **11** 1–11
- Ault T R, Cole J E and George S St 2012 The amplitude of decadal to multidecadal variability in precipitation simulated by state-of-the-art climate models *Geophys. Res. Lett.* **39** L21705
- Ault T R, Cole J E, Overpeck J T, Pederson G T, George S St, Otto-Bliesner B, Woodhouse C A and Deser C 2013 The continuum of hydroclimate variability in Western North America during the last millennium *J. Clim.* **26** 5863–78
- Baede A P M, Ahlonsou E, Ding Y and Schimel D 2001 *The Climate System: An Overview Climate Change 2001: The Scientific Basis* ed B Bolin and S Pollonais (Cambridge: Cambridge University Press)
- Bauer S E, Bausch A, Nazarenko L, Tsigaridis K, Xu B, Edwards R, Bisiaux M and McConnell J 2013 Historical and future black carbon deposition on the three ice caps: ice core measurements and model simulations from 1850 to 2100 *J. Geophys. Res.-Atmos.* **118** 7948–61
- Bistinas I, Harrison S P and Prentice J M C 2014 Causal relationships versus emergent patterns in the global controls of fire frequency *Biogeosciences* **11** 5087–101
- Capotondi A *et al* 2015 Understanding ENSO diversity *Bull. Am. Meteorol. Soc.* **96** 921–38
- Chen Y, Morton D C, Andela N, Giglio L and Randerson J T 2016 How much global burned area can be forecast on seasonal time scales using sea surface temperatures? *Environ. Res. Lett.* **11** 045001
- Chen Y, Morton D C, Jin Y, Collatz G J, Kasibhatla P S, van der Werf G R, DeFries R S and Randerson J T 2013 Long-term trends and interannual variability of forest, savanna and agricultural fires in South America *Carbon Manage.* **4** 617–38
- Chen Y, Randerson J T, Morton D C, DeFries R S, Collatz G J, Kasibhatla P S, Giglio L, Jin Y and Marlier M E 2011 Forecasting fire season severity in South America using sea surface temperature anomalies *Science* **334** 787–91
- Chikamoto Y, Timmermann A, Stevenson S, DiNezio P and Langford S 2015 Decadal predictability of soil water, vegetation, and wildfire frequency over North America *Clim. Dyn.* **45** 2213–35
- Chisholm R A, Wijedasa L S and Swinfield T 2016 The need for long-term remedies for Indonesia's forest fires *Conservation Biol.* **30** 5–6
- Clark S C, Ward D S and Mahowald N M 2015 The sensitivity of global climate to the episodicity of fire aerosol emissions *J. Geophys. Res. Atmos.* **120** 11589–607

- Dai A 2012 The influence of the inter-decadal Pacific oscillation on US precipitation during 1923–2010 *Clim. Dyn.* **41** 633–46
- Daniau A L *et al* 2012 Predictability of biomass burning in response to climate changes *Glob. Biogeochem. Cycles* **26** GB4007
- Duffy P A, Walsh J E, Graham J M, Mann D H and Rupp T S 2005 Impacts of large-scale atmospheric-ocean variability on Alaskan fire season severity *Ecol. Appl.* **15** 1317–30
- Dunne J P *et al* 2012 GFDL's ESM2 global coupled climate–carbon Earth system models: I. Physical formulation and baseline simulation characteristics *J. Clim.* **25** 6646–65
- Dunne J P *et al* 2013 GFDL's ESM2 global coupled climate–carbon earth system models: II. Carbon system formulation and baseline simulation characteristics *J. Clim.* **26** 2247–67
- Emile-Geay J, Cobb K, Mann M and Wittenberg A T 2013 Estimating central equatorial Pacific SST variability over the past millennium: II. Reconstructions and implications *J. Clim.* **26** 2329–52
- Falk D A, Heyerdahl E K, Brown P M, Farris C, Fule P Z, McKenzie D, Swetnam T W, Taylor A H and Van Horne M L 2011 Multi-scale controls of historical forest-fire regimes: new insights from fire-scar networks *Front. Ecol. Environ.* **9** 446–54
- Findell K L and Delworth T L 2010 *J. Clim.* **23** 485–503
- Flannigan M D, Krawchuk M A, de Groot W J, Wotton B M and Gowman L M 2009 Implications of changing climate for global wildland fire *Int. J. Wildland Fire* **18** 483–507
- Frolking S, Talbot J, Jones M C, Treat C C, Kauffman J B, Tuittila E-S and Roulet N 2011 Peatlands in the Earth's 21st century climate system *Environ. Rev.* **19** 371–96
- Giglio L, Randerson J T and van der Werf G R 2013 Analysis of daily, monthly, and annual burned area using the fourth-generation global fire emissions database (GFED4) *J. Geophys. Res.: Biogeosci.* **118** 317–28
- Hess J C, Scott C A, Hufford G L and Fleming M D 2001 El Niño and its impact on fire weather conditions in Alaska *Int. J. Wildland Fire* **10** 1–13
- Heyerdahl E K, McKenzie D, Daniels L D, Hessl A E, Littell J S and Mantua N J 2008 Climate drivers of regionally synchronous fires in the inland northwest (1651–1900) *Int. J. Wildland Fire* **17** 40–9
- Hurrell J W *et al* 2013 The community Earth system model: a framework for collaborative research *Bull. Am. Meteorol. Soc.* **94** 1339–60
- Hurt G C *et al* 2011 Harmonization of land-use scenarios for the period 1500–2100: 600 years of global gridded annual land-use transitions, wood harvest, and resulting secondary lands *Clim. Change* **109** 117–61
- Kaiser J W *et al* 2012 Biomass burning emissions estimated with a global fire assimilation system based on observed fire radiative power *Biogeosciences* **9** 527–54
- Kay J E *et al* 2015 The community Earth system model (CESM) large ensemble project: a community resource for studying climate change in the presence of internal climate variability *Bull. Am. Meteorol. Soc.* **96** 1333–49
- Kelly R, Chipman M L, Higuera P E, Stefanova I, Brubaker L B and Hu F S 2013 Recent burning of boreal forests exceeds fire regime limits of the past 10 000 years *Proc. Natl Acad. Sci.* **110** 13055–60
- Kipfmüller K F, Larson E R and George S St 2012 Does proxy uncertainty affect the relations inferred between the Pacific Decadal Oscillation and wildfire activity in the western United States? *Geophys. Res. Lett.* **39** L04703
- Kitzberger T, Brown P M, Heyerdahl E K, Swetnam T W and Veblen T T 2007 Contingent Pacific–Atlantic Ocean influence on multicentury wildfire synchrony over western North America *Proc. Natl Acad. Sci.* **104** 543–8
- Kloster S, Mahowald N M, Randerson J T, Thornton P E, Hoffman F M, Levis S, Lawrence P J, Feddema J J, Oleson K W and Lawrence D M 2010 Fire dynamics during the 20th century simulated by the Community Land Model *Biogeosciences* **7** 1877–902
- Knight J R, Folland C K and Scaife A A 2006 Climate impacts of the Atlantic multidecadal oscillation *Geophys. Res. Lett.* **33** L17706
- Knorr W, Jiang L and Arneeth A 2016 Climate, CO₂ and human population impacts on global wildfire emissions *Biogeosciences* **13** 267–82
- Lasslop G and Kloster S 2015 Impact of fuel variability on wildfire emission estimates *Atmos. Environ.* **121** 93–102
- Lawrence P J *et al* 2012 Simulating the biogeochemical and biogeophysical impacts of transient land cover change and wood harvest in the community climate system model (CCSM4) from 1850 to 2100 *J. Clim.* **25** 3071–95
- Le Page Y, Morton D, Bond-Lamberty B, Pereira J M C and Hurtt G 2015 HESFIRE: a global fire model to explore the role of anthropogenic and weather drivers *Biogeosciences* **12** 887–903
- Le Page Y, Pereira J M C, Trigo R, da Camara C, Oom D and Mota B 2008 Global fire activity patterns (1996–2006) and climatic influence: an analysis using the World Fire Atlas *Atmos. Chem. Phys.* **8** 1911–24
- Li F, Levis S and Ward D S 2013 Quantifying the role of fire in the Earth system: I. Improved global fire modeling in the Community Earth System Model (CESM1) *Biogeosciences* **10** 2293–314
- Malyshev S, Shevliakova E, Stouffer R J and Pacala S W 2015 Contrasting local versus regional effects of land-use-change-induced heterogeneity on historical climate: analysis with the GFDL Earth System Model *J. Clim.* **28** 5448–69
- Marlier M E *et al* 2012 El Niño and health risks from landscape fire emissions in southeast Asia *Nat. Clim. Change* **3** 131–6
- Marlier M E, DeFries R, Pennington D, Nelson E, Ordway E M, Lewis J, Koplitz S N and Micklely L J 2014 Future fire emissions associated with projected land use change in Sumatra *Glob. Change Biol.* **21** 345–62
- Marlier M E, DeFries R S, Kim P S, Koplitz S N, Jacob D J, Micklely L J and Myers S S 2015 Fire emissions and regional air quality impacts from fires in oil palm, timber, and logging concessions in Indonesia *Environ. Res. Lett.* **10** 085005
- Marlon J R, Bartlein P J, Carcaillet C, Gavin D G, Harrison S P, Higuera P E, Joos F, Power M J and Prentice I C 2008 Climate and human influences on global biomass burning over the past two millennia *Nat. Geosci.* **1** 697–702
- McGregor S, Timmermann A, England M H, Elison Timm O and Wittenberg A T 2013 Inferred changes in El Niño-southern oscillation variance over the past six centuries *Clim. Past* **9** 2269–84
- Meehl G A 2015 Decadal climate variability and the early-2000s hiatus *US CLIVAR Variations* ed D Menemenlis and J Sprintall **13** 1–6
- Meehl G A, Hu A and Santer B D 2009 The Mid-1970s climate shift in the Pacific and the relative roles of forced versus inherent decadal variability *J. Clim.* **22** 780–92
- Mieville A, Granier C, Liouise C, Guillaume B, Mouillot F, Lamarque J-F, Gregoire J-M and Petron G 2010 Emissions of gases and particles from biomass burning using satellite data and an historical reconstruction *Atmos. Environ.* **44** 1469–77
- Mo K C, Schemm J-K E and Yoo S-H 2009 Influence of ENSO and the Atlantic multidecadal oscillation on drought over the United States *J. Clim.* **22** 5962–82
- Monks S A, Arnold S R and Chipperfield M P 2012 Evidence for El Niño-southern oscillation (ENSO) influence on Arctic CO interannual variability through biomass burning emissions *Geophys. Res. Lett.* **39** L14804
- Mouillot F and Field C B 2005 Fire history and the global carbon budget: a 10x 10 fire history reconstruction for the 20th century *Glob. Change Biol.* **11** 398–420
- Naik V, Mauzerall D, Horowitz L, Schwarzkopf M D, Ramaswamy V and Oppenheimer M 2005 Net radiative forcing due to changes in regional emissions of tropospheric ozone precursors *J. Geophys. Res.* **110** D24306
- Nepstad D *et al* 2006 Inhibition of Amazon deforestation and fire by parks and indigenous lands *Conservation Biol.* **20** 65–73
- Nevison C D, Mahowald N M, Doney S C, Lima I D, van der Werf G R, Randerson J T, Baker D F, Kasibhatla P and

- McKinley G A 2008 Contribution of ocean, fossil fuel, land biosphere, and biomass burning carbon fluxes to seasonal and interannual variability in atmospheric CO₂ *J. Geophys. Res.* **113** G01010
- Pechony O and Shindell D T 2010 Driving forces of global wildfires over the past millennium and the forthcoming century *Proc. Natl Acad. Sci.* **107** 19167–70
- Pfeiffer M, Spessa A and Kaplan J O 2013 A model for global biomass burning in preindustrial time: LPJ-LMfire (v1.0) *Geosci. Model Dev.* **6** 643–85
- Phillips A S, Deser C and Fasullo J 2014 Evaluating modes of variability in climate models *Eos* **95** 453–5
- Power M J *et al* 2008 Changes in fire regimes since the Last Glacial Maximum: an assessment based on a global synthesis and analysis of charcoal data *Clim. Dyn.* **30** 887–907
- Prentice I C, Kelley D I, Foster P N, Friedlingstein P, Harrison S P and Bartlein P J 2011 Modeling fire and the terrestrial carbon balance *Glob. Biogeochem. Cycles* **25** GB3005
- Randerson J T *et al* 2006 The impact of boreal forest fire on climate warming *Science* **314** 1130–2
- Rayner N A, Parker D E, Horton E B, Folland C K, Alexander L V, Rowell D P, Kent E C and Kaplan A 2003 Global analyses of sea surface temperature, sea ice, and night marine air temperature since the late nineteenth century *J. Geophys. Res.* **108** 4407
- Rogers B M, Soja A J, Goulden M L and Randerson J T 2015 Influence of tree species on continental differences in boreal fires and climate feedbacks *Nat. Geosci.* **8** 228–34
- Sátori G, Williams E and Lemperger I 2009 Variability of global lightning activity on the ENSO time scale *Atmos. Res.* **91** 500–7
- Shevliakova E, Pacala S W, Malyshev S, Hurtt G C, Milly P C D, Caspersen J P, Sentman L T, Fisk J P, Wirth C and Crevoisier C 2009 Carbon cycling under 300 years of land use change: importance of the secondary vegetation sink *Glob. Biogeochem. Cycles* **23** GB2022
- Skinner W R, Shabbar A, Flannigan M D and Logan K 2006 Large forest fires in Canada and the relationship to global sea surface temperatures *J. Geophys. Res.* **111** D14106
- Taylor A H, Trouet V and Skinner C N 2008 Climatic influences on fire regimes in montane forests of the southern Cascades, California, USA *Int. J. Wildland Fire* **17** 60–71
- Thonicke K, Venesky S, Sitch S and Cramer W 2001 The role of fire disturbance for global vegetation dynamics: coupling fire into a dynamic global vegetation model *Glob. Ecol. Biogeogr.* **10** 661–7
- Tosca M G, Diner D J, Garay M J and Kalashnikova O V 2015 Human-caused fires limit convection in tropical Africa: first temporal observations and attribution *Geophys. Res. Lett.* **42** 6492–501
- Trenberth K E and Shea D J 2006 Atlantic hurricanes and natural variability in 2005 *Geophys. Res. Lett.* **33** L12704
- Trouet V, Taylor A H, Wahl E R, Skinner C N and Stephens S L 2010 Fire-climate interactions in the American West since 1400 CE *Geophys. Res. Lett.* **37** L04702
- van der Werf G R, Randerson J T, Collatz G J, Giglio L, Kasibhatla P S, Arellano A F, Olsen S C and Kasibhatla E S 2004 Continental-scale partitioning of fire emissions during the 1997–2001 El Niño/La Niña period *Science* **303** 73–6
- van der Werf G R, Randerson J T, Giglio L, Collatz G J, Kasibhatla P S and Arellano A F 2006 Interannual variability in global biomass burning emissions from 1997 to 2004 *Atmos. Chem. Phys.* **6** 3423–41
- van der Werf G R, Randerson J T, Giglio L, Gobron N and Dolman A J 2008 Climate controls on the variability of fires in the tropics and subtropics *Glob. Biogeochem. Cycles* **22** GB3028
- Venevsky S 2001 Broad-scale vegetation dynamics in north-eastern Eurasia—observations and simulations *PhD Thesis* Universität für Bodenkultur, Vienna 150 pp
- Voulgarakis A, Marlier M E, Faluvegi G, Shindell D T, Tsigaridis K and Mängeon S 2015 Interannual variability of tropospheric trace gases and aerosols: the role of biomass burning emissions *J. Geophys. Res.* **120** 7157–73
- Ward D S, Kloster S, Mahowald N M, Rogers B M, Randerson J T and Hess P G 2012 The changing radiative forcing of fires: global model estimates for past, present and future *Atmos. Chem. Phys.* **12** 10857–86
- Ward D S and Mahowald N M 2015 Local sources of global climate forcing from different categories of land use activities *Earth Syst. Dyn.* **6** 175–94
- Wiedinmyer C, Akagi S K, Yokelson R J, Emmons L K, Al-Saadi J A, Orlando J J and Soja A J 2011 The fire inventory from NCAR (FINN): a high resolution global model to estimate the emissions from open burning *Geosci. Model Dev.* **4** 625–41
- Wittenberg A T 2009 Are historical records sufficient to constrain ENSO simulations? *Geophys. Res. Lett.* **36** L12702
- Wittenberg A T 2015 Low-frequency variations of ENSO *US CLIVAR Variations* ed A Kumar and Y Xue **13** 26–31
- Wittenberg A T, Rosati A, Delworth T L, Vecchi G A and Zeng F 2014 ENSO modulation: is it decadal predictable? *J. Clim.* **27** 2667–81
- Yang J, Tian H, Tao B, Ren W, Kush J, Liu Y and Wang Y 2014 Spatial and temporal patterns of global burned area in response to anthropogenic and environmental factors: reconstructing global fire history for the 20th and early 21st centuries *J. Geophys. Res. Biogeosci.* **119** 249–63
- Yue C *et al* 2014 Modelling the role of fires in the terrestrial carbon balance by incorporating SPITFIRE into the global vegetation model ORCHIDEE: I. Simulating historical global burned area and fire regimes *Geosci. Model Dev.* **7** 2747–67
- Zennaro P *et al* 2014 Fire in ice: two millennia of boreal forest fire history from the Greenland NEEM ice core *Clim. Past* **10** 1905–24